

Multiphysics Coupling Effect on Interfacial Properties of CNT/GFRP/CFRP Composites for Electrothermal Anti-/de-icing Applications

Xudan Yao[1,2,*], Yaqi Wang[1], Haolin Wang[1] & Yaxin Wang[1]

[1]School of Aeronautics, Northwestern Polytechnical University, Xi'an 710072, China
[2] National Key Laboratory of Strength and Structural Integrity, Xi'an 710072, China
*Corresponding author: x.yao@nwpu.edu.cn

Abstract

With the increasing use of composites in aerostructures owing to the lightweight and design flexibility, multifunctional structures have drawn much attention for integrated design. Carbon nanotubes (CNTs) could be integrated into the carbon fibre reinforced polymer (CFRP) composite aerostructures for electrothermal anti-/de-icing. Among which, electrical insulation layer should be applied to prevent the short circuit, and glass fibre reinforced polymer (GFRP) composites were employed. However, the thermal and moisture mismatch between different plies and materials will lead to property degradation due to the multiphysics coupling effect. CNT/GFRP/CFRP composites with different thermal cycles between -55 ℃ and +80 ℃ were studied in this work, to simulate the anti-/de-icing service conditions. Up to 10,000 thermal cycles, as well as hygrothermal aging and thermo-hygro-mechanical coupling environment, have been applied to the composites, with the interlaminar shear strength (ILSS) evaluated periodically. Fickian model fits the moisture absorption curves well for both hygrothermal and thermo-hygro-mechanical coupling environments. The composites exhibit excellent thermal stability under thermal cycling, with 89% ILSS maintained after 10,000 cycles. However, with additional moisture and mechanical loading applied, the strength degraded largely due to the deteriorated interfacial properties.

Keywords: thermal cycling, hygrothermal aging, thermo-hygro-mechanical coupling, CNT/GFRP/CFRP composites, interfacial properties

1. Introduction

When an aircraft flies in cold and cloudy environments, ice may form on its leading edges and affect the aerodynamic performance and threat the flight safety [1]. Meanwhile, carbon fibre reinforced polymer (CFRP) composites are widely used in the primary structures of the new-generation passenger aircraft, owing to their exceptional specific strength and stiffness. Anti-icing/de-icing (AI/DI) is vital for flight safety, which is conventionally achieved by hot air bleed systems, while facing new challenges for the latest generation aircraft with composite wings due to their relatively low thermal conductivity. Electro-thermal systems are promising alternatives, owing to their high energy efficiency, low maintenance requirements and the absence of bleed exhaust holes [2,3]. In particular, CFRPs integrated with heating elements, such as carbon nanotubes (CNTs) embedded within electrical insulators like glass fibre reinforced plastics (GFRPs), was thought as one promising candidate for aerostructures with AI/DI functions [2-7]. However, the difference of thermal expansion and moisture absorption between different layers and components, will lead to internal stresses under service conditions, and as a result, the strength of the composites will be affected.

As shown in Figure 1a, during the flight, the aircraft will experience temperatures ranging from -55 ℃ to 20 ℃ due to the external static air [8]. Among which, -20 ℃ to 10 ℃ possess the highest risk of ice accretion, and with the AI/DI system switched on, the temperature will be increased to 80 ℃ [9,10]. In combination, the temperature range for the thermal cycling is set from -55 ℃ to 80 ℃ (Figure

1b) in this work.

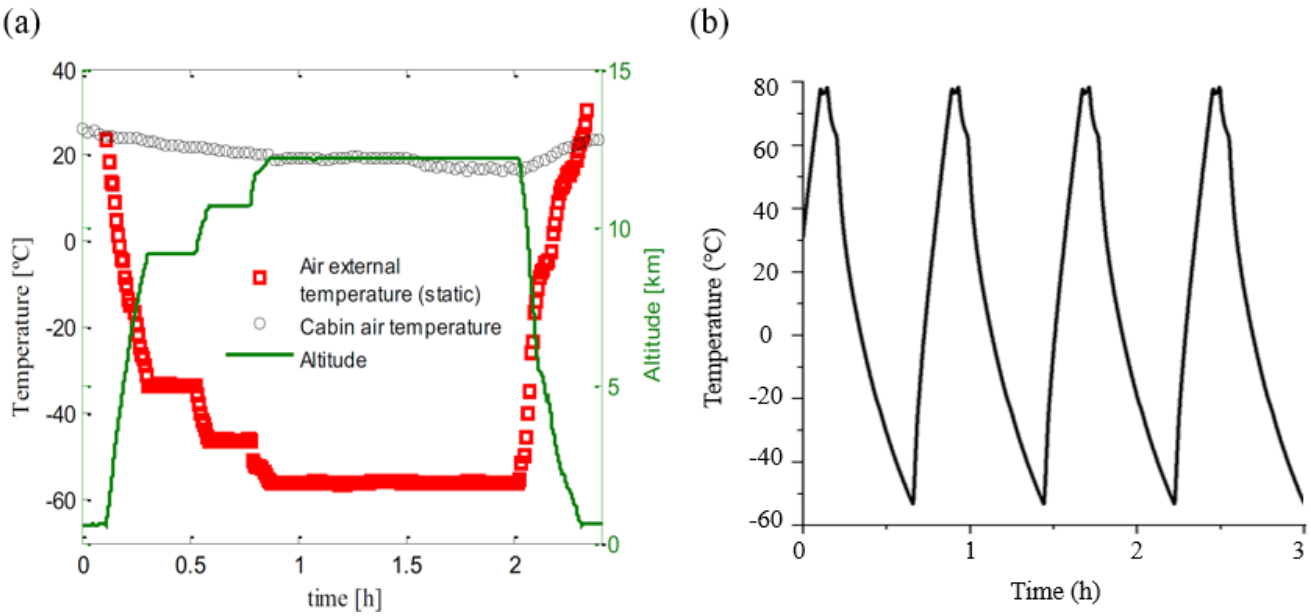


Figure 1 (a) Temperature profile during the flight [8]. (b) Thermal cycles for the CNT/GFRP/CFRP composites.

In addition, different components have different moisture absorption performance which will superimpose the wet expansion difference. Meanwhile, higher temperatures and additional mechanical loading will accelerate the movement of water molecules, resulting in an increased amount of moisture absorption which will lead to matrix plasticization, swelling, and results in a more severe degradation of the interfacial properties of the composites. Afterwards, the interlaminar shear strength (ILSS) of composite laminates will be studied to evaluate the influence of thermal cycling, hygrothermal aging and thermo-hygro-mechanical coupling on the composites.

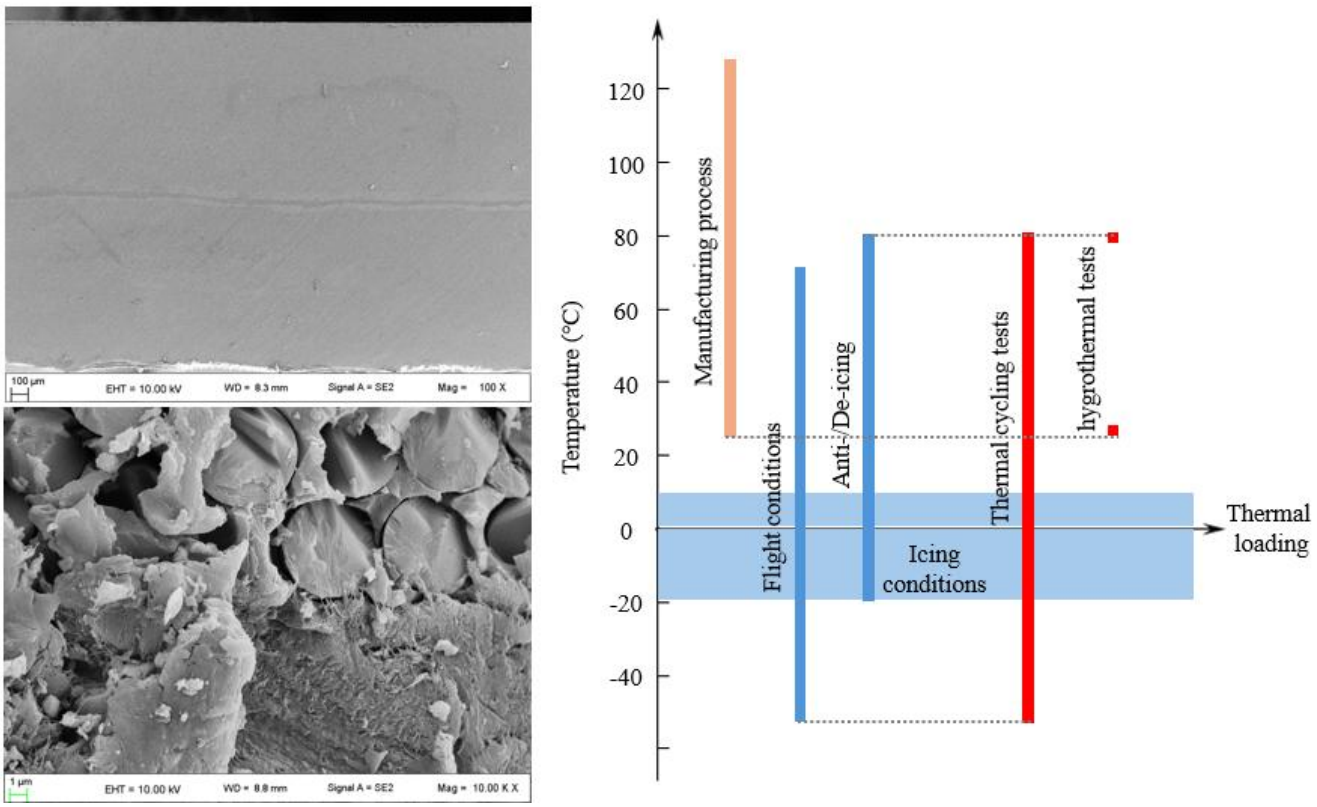
2. Experimental

2.1 Materials and fabrication

Unidirectional (UD) T700 carbon fibre/epoxy prepreg (290 g/m^2) and plain weave glass fibre/epoxy prepreg (39 g/m^2) were supplied by Weihai Guangwei Composites Co Ltd, China. CNT films were fabricated by the floating catalyst chemical vapor deposition (FCCVD) method at the Suzhou Institute of Nano-Tech and Nano-Bionics, Chinese Academy of Sciences [11,12]. Woven glass fiber prepregs were designed to wrap the CNT films, working as the electrical insulator, and then the whole assembly was embedded in the middle of unidirectional (0°) carbon fiber prepregs. After the layup, the composite was cured in an autoclave, and the thickness of the cured composite is at around 2 mm. The cross-sectional SEM images are shown in Figure 2a, indicating the symmetric layup, and the interface between the CNT film and GFRP shows that carbon nanotubes work as bridges that help connecting the glass fibre and epoxy matrix.

2.2 Environmental tests

Apart from the manufacturing procedure with the temperature range from room temperature to 130 ℃, the aircraft experiences flight conditions, icing conditions and anti-/de-icing [7,13], as shown in Figure 2b. the overall temperature range of the cyclic thermal loading was set as -55~80 ℃. An environmental chamber (GWS, HSL-02JA) was used to conduct the thermal cycles, as shown in Figure 1b, with each cycle duration of 47 min. Additionally, moisture absorption differences of different components will superimpose the wet expansion difference, hygrothermal synergism causes matrix plasticization, swelling, and results in a more severe degradation of the interfacial properties of the composites. Effects of the hygrothermal aging and thermo-hygro-mechanical coupling are also under investigation.



(a) (b)

Figure 2 (a) SEM images of the cross section of the CNT/GFRP/CFRP composite and (b) its thermal and hygrothermal loading conditions.

2.3 Interlaminar shear tests

To evaluate the interlaminar shear strength (ILSS), double beam shear (DBS) tests of composite samples before and after thermal cycling and hygrothermal aging were performed using an electronic universal testing machine, following the ISO 19927:2018 standard [14], with a high-speed camera was employed to continuously capture images of cross-sectional surface, with a frequency of 1 Hz. The specimen is 30 mm in length, 10 mm ± 0.2 mm in width, and 2 mm ± 0.1 mm in thickness, and the ILSS (τ_{13max}) is calculated using the equation (Eq. 3):

$$\tau_{13max} = 33F_{crit} / 64bh \quad (1)$$

where F_{crit} is the critical load when delamination failure occurs, b and h are the specimen width and thickness respectively, which were measured for each specimen before the tests.

3. Results and discussion

To promote the dominance of interlaminar shear stresses in the composites, and study the interlaminar behaviour of the CNT/GFRP/CFRP, double beam shear tests were applied to composite specimens after different environmental tests. The representative load-displacement curve of DBS tests is shown in Figure 3, where the critical load is the load with crack initiation. During the tests, delamination occurred consistently within one of the nearly pure interlaminar shear regions of the specimen where has minimum bending stresses. During the whole procedure, delamination dominates the failure, fulfills the acceptable failure modes of the standard and could be used to evaluate the interlaminar properties of the composite laminates.

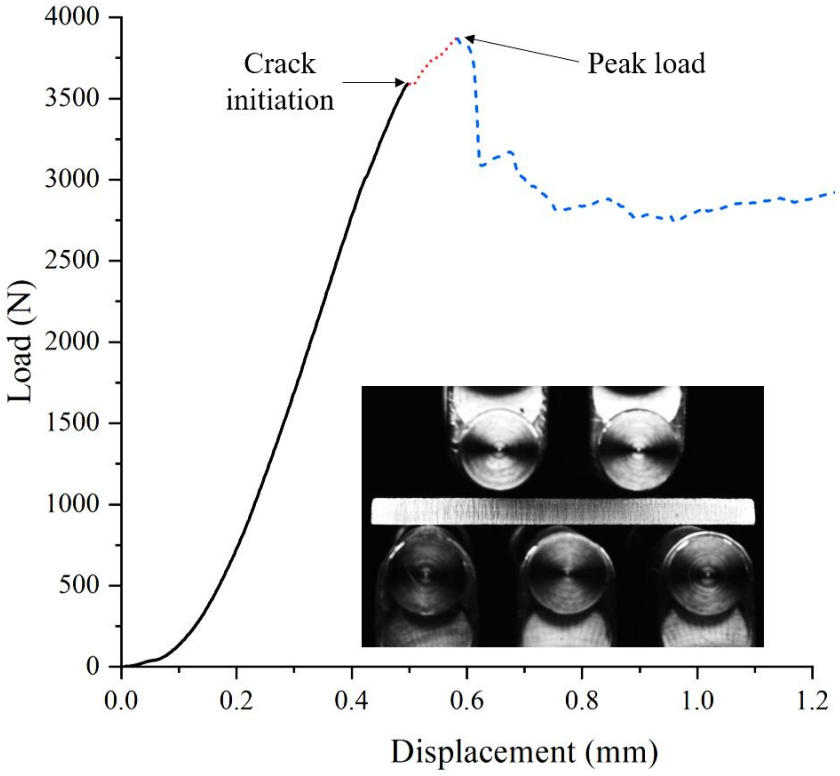


Figure 3 Representative load-displacement curve of the DBS test, with the embedded image showing the testing setup.

3.1 Effect of thermal cycling

CNT/GFRP/CFRP composites after different number of thermal cycles have been tested, with the ILSS relative values summarized and plotted in Figure 4. Thermal cycling of the specimens between -55 ℃ and +80 ℃ led to reductions of the ILSS values by 1.4%, 4.0%, 5.5% and 10% after 100, 500, 1,000 and 2,000 cycles, as a result of the thermal mismatch. While with the number of cycles further increased, the residual strength stabilized at around 89% of the original value even after 10,000 cycles, indicating the robust thermal stability.

To evaluate the strength degradation of the CNT/GFRP/CFRP composites due to thermal fatigue, Bulmanis et al model [15] is used to fit the experimental results.

$$S = S_0 + \eta(1-e^{-\lambda n}) - \beta\ln(1+\alpha n) \quad (2)$$

$$100 \times S/S_0 = 100 + a(1-e^{-\lambda n}) - b\ln(1+\alpha n) \quad (3)$$

where S and S_0 are the strength before and after the thermal fatigue, η and β are material properties, λ and α represent parameters of the material and the ambient medium, n is the number of thermal cycling. After the non-linear analysis, as shown in Figure 4, fitting parameters were obtained for the Bulmanis et al model with the R^2 of 0.93, and summarized in Table 1.

Table 1. Model fitting parameters for thermal cycling

a	λ	b	α
-8.69	0.001	2.26	0.005

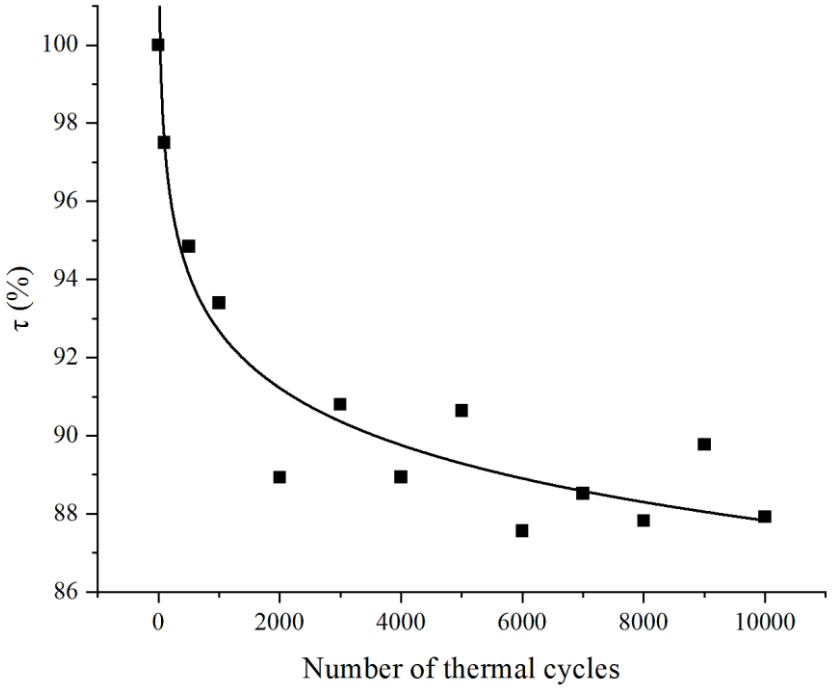
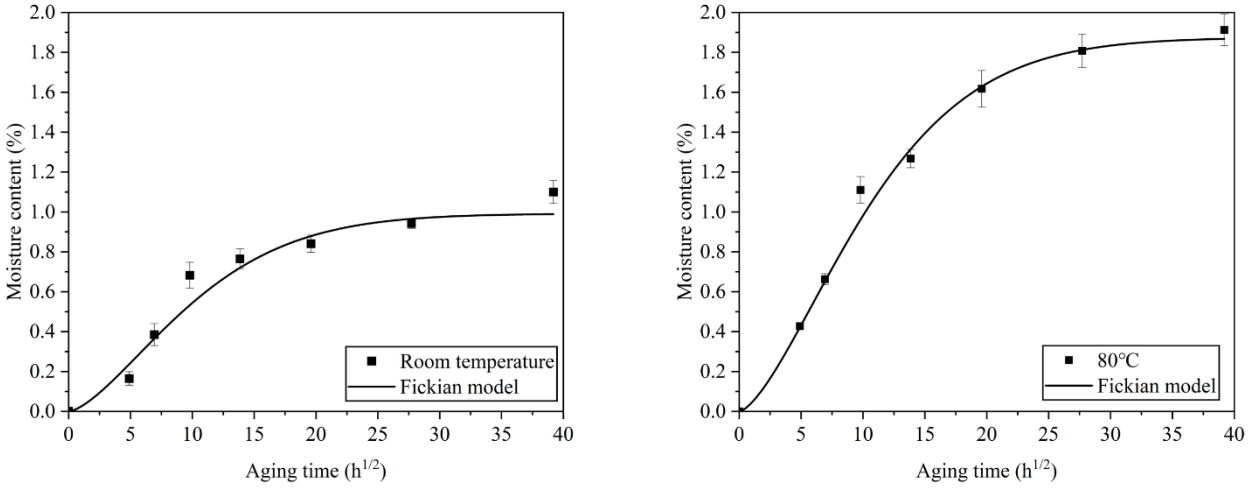


Figure 4 ILSS (interlaminar shear strength) values with the fitted curve of CNT/GFRP/CFRP composites after different thermal cycles

3.2 Effect of hygrothermal aging

The moisture contents of CNT/GFRP/CFRP composites during water immersion aging at room temperature and 80 °C were periodically recorded and summarized in Figure 5. For both conditions, the moisture content increased rapidly at the initial stage and then gradually approached saturation, with the Fickian model well fitted. Compared with the room-temperature specimens, composites aged at the elevated temperature of 80 °C exhibited higher moisture absorption rates and saturated moisture content. The saturated moisture content reached approximately 1.9% at 80 °C, compared with 1.1% at room temperature, indicating that elevated temperature promoted moisture diffusion inside the composites.



(a) (b)

Figure 5 Moisture absorption curves of CNT/GFRP/CFRP composites at (a) room temperature and (b) 80 ℃

The ILSS values of CNT/GFRP/CFRP composites after different hygrothermal aging times were summarized and plotted in Figure 6. With increasing aging time, the ILSS continuously decreased, and the strength degradation was more pronounced at 80 °C. After 64 days of water immersion at

room temperature, the ILSS decreased by approximately 17.6%, while a reduction of more than 50% was obtained after aging at 80 °C. This indicates that the high-temperature water immersion environment significantly increased moisture penetration, matrix plasticization and interfacial damage accumulation, leading to rapid degradation of the interfacial properties of the composites.

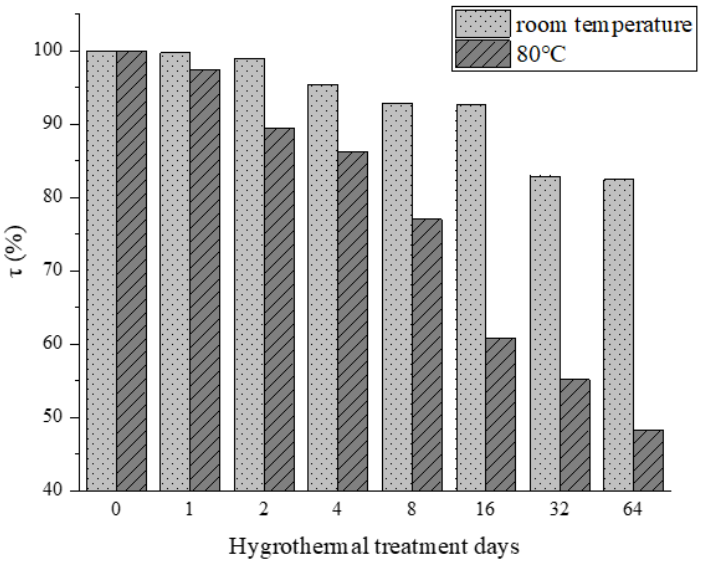


Figure 6 ILSS of CNT/GFRP/CFRP composites after hygrothermal aging, relative values compared with the reference (non-cycled)

3.3 Effect of thermo-hygro-mechanical coupled environment

The moisture absorption behaviour of CNT/GFRP/CFRP composites under hygrothermal environment with different sustained static loading conditions were investigated, with the results summarized and plotted in Figure 7. Under both 30% and 60% static loadings, the moisture content increased gradually with the number of hygrothermal cycles and then tended to stabilize, showing typical Fickian-type diffusion characteristics. Compared with the 30% static loading condition, specimens under 60% static loading exhibited higher moisture content throughout the hygrothermal cycling process. After 600 cycles, the moisture content reached approximately 1.7% under 60% static loading, compared with around 1.3% under 30% static loading. This indicates that a higher loading level significantly promoted the diffusion and transport of water molecules inside the composites, resulting in higher moisture uptake under the thermal-hygro-mechanical coupling environment.

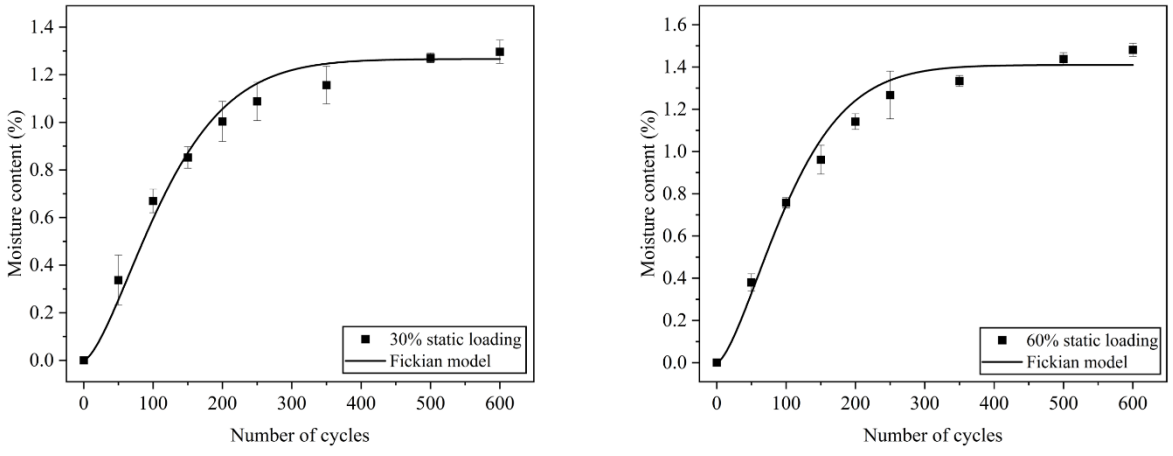


Figure 7 Moisture absorption curves of CNT/GFRP/CFRP composites under (a) 30% and (b) 60%

mechanical loadings

The relative ILSS values of CNT/GFRP/CFRP composites under different sustained static loading levels are summarized and plotted in Figure 8. With increasing number of hygrothermal cycles, the relative ILSS continuously decreased, and the degradation under 60% static loading was more pronounced than that under 30% static loading. After 600 hygrothermal cycles, the residual strengths under 30% and 60% static loadings were approximately 65.1% and 58.8%, respectively. This demonstrates that the coupling effect of static loading and hygrothermal cycling significantly weakened the interfacial load-bearing capacity of the composites, and a higher loading level led to more severe interfacial degradation. Sustained static loading promoted interfacial stress concentration and microcrack propagation, while accelerating moisture penetration along matrix cracks and fiber/matrix interfaces. As a result, matrix plasticization, interfacial debonding, and reduction in load transfer efficiency were further intensified, eventually leading to a significant decrease in interlaminar shear strength.

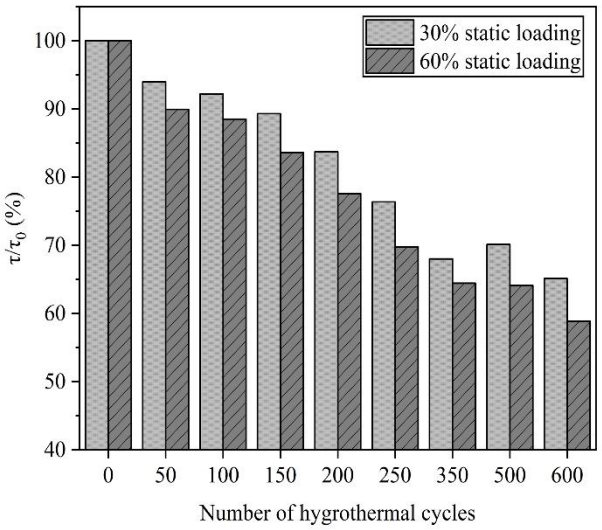


Figure 8 ILSS of CNT/GFRP/CFRP composites under thermo-hygro-mechanical coupled environment after different hygrothermal cycles

4. Conclusions

CNT/GFRP/CFRP composites that can be used for electrothermal anti-icing and de-icing were subjected to thermal cycling between -55 ℃ and +80 ℃, as well as hygrothermal aging at both room temperature and 80 ℃, also with additional static loadings, to investigate the influence of service environment on their interfacial properties. Double beam shear tests with minimal axial bending stress were employed, the delamination dominated failures were achieved as a result of the interlaminar shear. For the thermal cycling with a temperature range of -55 ℃ to 80 ℃, the ILSS of the composite decreased at first and then stabilized with a residual strength of ~89% even after 10,000 cycles, indicating appropriate thermal stability. The degradation during thermal cycling can be evaluated based on the Bulmanis model, which could be used to predict the strength degradation of the composites during thermal fatigue. However, hygrothermal aging and thermo-hygro-mechanical coupling effect degraded the strength largely due to the deteriorated interfacial properties.

In addition, among all the thermal cycling and hygrothermal aging tests, no obvious debonding was observed in the CNT region, owing to the flexibility of CNTs that could be potentially applied to improve the interfacial properties. It indicates that the CNT-based electrothermal heating element has excellent stability and compatibility with FRP composites.

Acknowledgments

This work was supported by the National Natural Science Foundation of China (Grants No. 52302457).

Copyright Statement

The authors confirm that they, and/or their company or organization, hold copyright on all of the original material included in this paper. The authors also confirm that they have obtained permission, from the copyright holder of any third party material included in this paper, to publish it as part of their paper. The authors confirm that they give permission, or have obtained permission from the copyright holder of this paper, for the publication and distribution of this paper as part of the ICAS proceedings or as individual off-prints from the proceedings.

References

[1] Cao Y, Tan W and Wu Z. Aircraft icing: An ongoing threat to aviation safety. *Aerospace Science and Technology*, 75:353–385, 2018.

[2] Yao X, Hawkins SC and Falzon BG. An advanced anti-icing/de-icing sys-tem utilizing highly aligned carbon nanotube webs. *Carbon*, 136:130-138, 2018.

[3] Yao X, Falzon BG, Hawkins SC and Tsantzalis S. Aligned carbon nano-tube webs embedded in a composite laminate: A route towards a highly tunable electro-thermal system. *Carbon*, 129:486-494, 2018.

[4] Yao X, Hawkins SC and Falzon BG. Orthotropic Electro-Thermal Behaviour of Highly-aligned Carbon Nanotube Web Based Composites. *Composites Science and Technology*, 170:157-164, 2019.

[5] Yao X, Hawkins SC and Falzon BG. A Repairable and Flexible Carbon Nanotube Web Based Electro-Thermal System. *The Aeronautical Journal*, 125 (1292):1833-1843, 2021.

[6] Ying Y, Lu H, Yang Q, Wang Q, Si Y, Feng Y, Wang W and Yao X. Advances in electrothermal anti-icing and de-icing techniques for aircraft. *Acta Materiae Compositae Sinica*, 44(0): 1-24 (in Chinese), 2025.

[7] Wang Y, Wang H, Wang W, Lyu W, Si Y and Yao X. Effect of thermal cycling and hygrothermal aging on interfacial properties of CNT/GFRP/CFRP composites for electrothermal anti-icing/de-icing applications. *Composites Communications*, 64, 102781, 2026.

[8] Oliveira JLG, Tecchio C, Paiva KV, Mantelli MBH, Gandolfi R and Ribeiro LGS. In-flight testing of loop thermosyphons for aircraft cooling. *Applied Thermal Engineering*, 98:144–156, 2016.

[9] Hagenbeek M, Dias MM, Sinke J and Jansen K. Creep behaviour of FM906 glass-fibre epoxy as used in heated fibre metal laminates. *Journal of Composite Materials*, 53:3829-3840, 2019.

[10] Federal Aviation Administration (FAA). Airplane and engine certification requirements in supercooled large drop, mixed phase and ice crystal icing conditions. *Federal Register* 75:37311–37339, 2010.

[11] Xu X, Zhang Y, Jiang J, Wang H, Zhao X, Li Q and Lu W. In-situ curing of glass fiber reinforced polymer composites via resistive heating of carbon nanotube films. *Composites Science and Technology,* 149:20–27, 2017.

[12] Xu H, Tong X, Zhang Y, Li Q and Lu W. Mechanical and electrical properties of laminated composites containing continuous carbon nanotube film interleaves. *Composites Science and Technology, 127:113–118, 2016.*

[13] Müller B, Hagenbeek M and Sinke J. Thermal cycling of (heated) fibre metal laminates. *Composite Structures,* 152:106–116, 2016.

[14] Fibre-reinforced plastic composites —Determination of interlaminar strength and modulus by double beam shear test. *BS ISO* 19927:2018.

[15] Bulmanis VN, Gunyaev GM, Krivonos VV, Mashinskaya GP, Merkulova VM, Milyutin GI, Gerasimov AA and Kuzmin SA. Atmospheric durability of polymer-fiber composites in cold climates. *Mechanics of Composite Materials*, 27:698-705, 1991.